Correlations between rheological and mechanical properties of fructo-polysaccharides extracted from Ornithogalum billardieri as biobased adhesive for biomedical applications

Mohammad Kazem Medlej, Simon Le Floc'h, Céline Pochat-Bohatier, Ghassan Nasser, Suming Li, Akram Hijazi

Correlations between rheological and mechanical properties of fructo-polysaccharides extracted from *Ornithogalum billardieri* as biobased adhesive for biomedical applications

Mohammad Kazem Medlej [a,b], Simon Le Floch [c], Ghassan Nasser [b], Suming Li [a,*], Akram Hijazi [b], Céline Pochat-Bohatier [a,*]

[a] *Institut Européen des Membranes, IEM UMR 5635, Univ Montpellier, CNRS, ENSCM, Montpellier, France*
[b] *Platform for Research and Analysis in Environmental Sciences (PRASE), Lebanese University, Beirut, Lebanon*
[c] *Laboratoire de Mécanique et Génie Civil (LMGC), UMR 5508, Univ Montpellier, CNRS, Montpellier, France*

Keywords:
Tissue adhesive
Polysaccharides
Rheological properties
Mechanical properties
Correlations

Polysaccharides are extracted from *Ornithogalum* by maceration using different ultrasound (US) treatment times (0%US, 50%US, 100%US), and under optimized extraction conditions (OP%US). The total carbohydrates content (TCC) and proteins content of the extracts were determined. Data show that the extraction parameters significantly influence the extracts composition. Rheological measurements allowed determining the liquid, intermediate and gel states of the extract's solutions. The adhesion strength of the solutions was evaluated on paper and polylactide (PLA) substrates to evaluate their potential as environmentally friendly adhesive. OP%US presents the highest adhesion strength (1418.3 kPa) on paper, and is further tested on pork skin substrates. The adhesion strength is higher on skin/paper (870 kPa) than on skin/skin (411 kPa) substrate due to the capillary force of paper which allows penetration of adhesive into the micropores of paper. The correlation between rheological properties and adhesion strength indicates that the adhesion strength strongly depends on the state of adhesives and the substrate type. SEM analyses show that higher adhesion strength (intermediate and gel states) involves both cohesive and adhesive failure, whereas only adhesive failure is observed in liquid state on PLA substrates. Therefore, these polysaccharides extracts could be very promising as tissue adhesive in medical applications.

1. Introduction

Synthetic adhesives generally present high adhesion strength which can reach 40 MPa in the case of the epoxy adhesives [1,2]. However, most of them are toxic and harmful to the human health and the environment because of the presence of volatile and highly reactive organic compounds such as epichlorohydrin, toluene, diisocyanate, and formaldehyde [3,4].

In recent years, the development of bio-based adhesives attracted more and more attention as they allow to avoid health hazards and environment pollution, as well as to reduce the dependency on petroleum resources [5]. Li et al. developed a mechanical approach to get insights into abalone adhesion on different types of surfaces, and found that the normal adhesion strength mainly stems from the suction pressure, van der Waals force, capillary force, and Stefan adhesion [6]. Liu et al. developed a unified analysis framework for the adhesion of an elastic system with movable boundaries [7]. Many studies showed that the adhesion strength is strongly related to the work of adhesion which is dependent on the surface energy and thus on the contact angle [8]. Nevertheless, currently there is no in-depth study on the effect of the rheological state of adhesives on the adhesion strength.

Polysaccharides generally present good biocompatibility, biodegradability, and mechanical properties, which allowed applications as medical dressing and bio-adhesives, including adhesives for wood, plant particles, glass, and metal [9,10]. Nevertheless, the adhesive strength of polysaccharides is much weaker than that of synthetic ones, which constrains their industrial applications. For example, Yamada et al. reported an adhesion strength of 400 kPa for chitosan reticulated with glutaraldehyde [9].

Polysaccharides are often associated with other compounds. The presence of proteins in cross-linked polysaccharide has major influence on the network structure [11], and can contribute to the adhesion

* Corresponding authors.
E-mail addresses: suming.li@umontpellier.fr (S. Li), celine.pochat@umontpellier.fr (C. Pochat-Bohatier).

strength and the stability of polysaccharides [12]. Yuan et al. obtained an optimal adhesion strength of 0.99 MPa for soybean polysaccharide conjugated to soy protein on plywood.

The adhesive properties of polysaccharides are closely related to their rheological behavior which depends on the basic characteristics such as polarity, hydrogen bonding, functional groups [13], and molecular weight and dispersity [14], on the chain structure such as chain lengths, degree and pattern of branching chains, and on the presence of heteromonomers [15–17]. The presence of carboxylates, ethers, and hydroxyls in the skeleton of polysaccharides increases the polarity and hydrogen bonding, which enhances the adhesion strength on metals and wood substrates. On the other hand, the presence of hydroxyl and carboxylate groups allows for noncovalent inter/intra chain interactions, chemical modification and cross-linking to improve the adhesion strength [18].

The most important properties of a tissue adhesive include mechanical strength, rheological behavior, biocompatibility, and biodegradability. The rheological behavior of a viscoelastic material is usually characterized by storage modulus (G′) and loss modulus (G″). The optimal adhesion strength can be achieved through the balancing between the elasticity and rigidity of adhesives. Whereas the cohesive and adhesive failure can be evaluated using the Scanning Electron Microscope analysis.

In our previous study, a new extraction process combining both ultrasound and maceration was optimized to extract polysaccharides from *Ornithogalum*, a non-edible wild plant widespread in Lebanon, using the Surface Response Methodology (RSM) [19]. The extracted polysaccharides were characterized by using ^{1}H,^{13}C, HSQC, HMBC, and COSY NMR analysis. The antioxidant activities and the biocompatibility of the extract were also examined to evaluate its potential for applications in the agro-food industry [20].

The aim of the present study was to elucidate the effect of extraction conditions on the extract's composition, rheological properties and adhesion strength. The adhesion strength and its correlation with the rheological behavior were investigated at different types of substrates in order to develop a new bio-based tissue adhesive for medical applications.

2. Materials and methods

2.1. Extraction

The polysaccharides were extracted from Ornithogalum by combination of maceration and sonication as previously reported [19]. Briefly, 1 g of the purified powder was added in 10 mL of ultrapure water. The mixture was homogenized for 30 s at 3500 rpm. Extraction was carried out using the ultrasound (Badelin SonoRex) at fixed frequency (35 kHz) and power (120 W) during 30 min at 25 °C. The time ratio of ultra-sonic treatment to the total extraction was 0%, 50%, and 100%, corresponding to 0, 15 and 30 min ultra-sonic treatment, respectively. The extracts were then obtained by precipitation in ethanol, followed by centrifugation at 6000 rmp for 15 min, and vacuum drying at 40 °C up to constant weight. The extract previously obtained under the optimal extraction conditions (extraction time 37.1 min, temperature 44.2 °C, water volume to mass ratio 33.8 mL/g, and US% 51.7%), namely OP% US, was comparatively studied [19].

2.2. Characterization of the extracts

2.2.1. Total carbohydrates content (TCC)

The TCC of the extracts was determined according to Dubois method [21]. A stock solution of extract at 2.5 mg/mL was prepared, and diluted 200 times. 500 µL of the diluted solution was mixed with 2.5 mL of concentrated H_2SO_4 and 500 µL of phenol at 5% w/w. After incubation for 10 min at 100 °C, the mixture was cooled down to room temperature for 20 min in the dark, and the absorbance was measured at 490 nm. The concentration of polysaccharides was obtained from a previously established calibration curve using glucose as standard. The TCC (%) was calculated using the following equation.

$$\mathrm{TCC}\ (\%) = \frac{W_P}{W_S} \times 100 \quad (1)$$

where W_P is the weight of polysaccharides, and W_P the weight of sample.

2.2.2. Protein content

The protein content of the extracts was determined according to Lowry method [22]. A stock of reagent solution was first prepared by mixing 2% (w/v) Na_2CO_3, 1% (w/v) $CuSO_4.5H_2O$, and 2% (w/v) sodium potassium tartrate at a volume ratio of 100:1:1. 0.1 mL of 2 N NaOH was added to 0.1 mL of sample solution, then the mixture was heated at 100 °C for 10 min in boiling water bath. After cooling down to room temperature, 1 mL of freshly prepared reagent was added to the mixture, followed by addition of 0.1 mL of Folin reagent (1 N) 10 min later. After homogenization, the solution was allowed to stand at room temperature for 30 min, and the absorbance was measured at 550 nm. The protein content was obtained from a standard curve previously established by using bovine serum albumin (BSA) as standard at concentrations ranging from 0.1 to 1.0 mg/mL [22].

2.3. Size-exclusion chromatography (SEC)

Size-exclusion chromatography (SEC) was carried out using HPLC (DW-LC1620A) equipped with TSK gel PW5000 + PW3000 columns and refraction index and ultraviolet detectors. The temperature of the columns and detectors was 20 and 35 °C, respectively. A pH 6 phosphate buffer at 10 mg/mL was used as eluent at a flow rate of 1 mL/min. Calibration was realized using pullulan standards with molar masses from 500 to 25,000 Da. Data were processed using OmniSEC software.

2.4. Rheological properties

Rheological experiments were performed with Physical MCR 301 Rheometer (Anton Paar). Measurements were made at 25 °C using a cone plate (cone of 1°, diameter of 50 mm). Silicone oil was applied to avoid water evaporation. The stress-shear sweep was done for solutions at different concentrations from 5 to 25% using a steady shear flow range from 0.01 to 1000 S^{-1}.

Angular frequency sweep was performed in the linear viscoelastic regime from 40 to 800 rad/s corresponding to a shear strain range from 0.01 to 70% at fixed angular frequency 10 rad/s.

2.5. Adhesion test

The international standard ISO 4587-03 describes a method that consists in determining the tensile lap-shear strength of rigid-to-rigid bonded assemblies. A single-overlap adhesive joint bond was stressed by application of a tensile force parallel to the bond area and to the major axis of the specimen in order to determine the adhesive force [23]. This standard was adopted with slight modification, using poly (lactic acid) (PLA) and paper (180 g/m^2) as substrates. The preparation of the samples was carried out as follows. The polysaccharides extract was dissolved in distilled water at desired concentrations to yield an adhesive, and a volume of 5 µL was deposited on the part to be bonded. Then, the adhesive was gently spread to homogeneously cover the entire bonding surface (40 mm^2). After that, the samples are dried at room temperature for 30 min under a pressure of 9.8 N on the adhesive.

Lap-shear standard test by tension loading ASTMF 2255-05 is used to determine the force of tissue adhesives [24]. The pork skin dermis excised from belly was used as biological substrate. After removal of non-dermal tissues by blunt dissection, all tissues were frozen rapidly, cleaned and thawed prior to testing. The dermis was cut in 10–14 mm

pieces. 5 μL of the adhesive was applied to one side of dermis. Then, it was overlapped by a second piece (Fig. 1). All the samples are kept moisturized and are tested 1 h after adhesive application. The crosshead speed was 10 mm·s^{-1}. For each test, the load versus displacement was measured, and the shear stress at break is used to characterize adhesion for each formulation. Each sample was tested at least seven times.

The tests of the adhesive formulations (0% US, 50% US, 100% US, OP %US) with various bonded assemblies (PLA/adhesive/PLA, paper/adhesive/paper, skin/adhesive/skin, and paper/adhesive/skin), were carried out by using Metravibe DMA 50 N, under static conditions where the force ramp as a function of time was fixed at 0.1 N/s. The data of all testes were recorded in real time using a software Computer-based analysis.

The used dimensions of the samples are as the following:

- Width l = 10 mm.
- Thickness E′ = 0.44 mm for PLA, 0.22 mm for paper.
- Length L = 14 mm.
- Contact length L′ = 4 mm.

The adhesion strength was calculated using the following equation.

$$\boldsymbol{\sigma_b} = \frac{F_b}{A} \quad (2)$$

where $\boldsymbol{\sigma_b}$ is the stress at break (kPa), F_b is the force at break (N), and A is the contact area (m^2).

2.6. Scanning electron microscopy (SEM)

The failure types and the effect of mechanical interlocking are determined by using scanning electron microscopy (SEM). The microstructures for the substrate after adhesion tests, and cleaning by hot presser air gun were analyzed using Zeiss EVOHD15 with a resolution of 1.9 nm at 30 kV.

2.7. Statistical analysis

All experiments were run in triplicate for the rheological tests, and 7 times for the tensile strength tests. Data are expressed as mean ± SD (standard deviation). A one-way analysis of variance (ANOVA) was then performed to estimate the significance. A value of $p < 0.05$ is considered statistically significant.

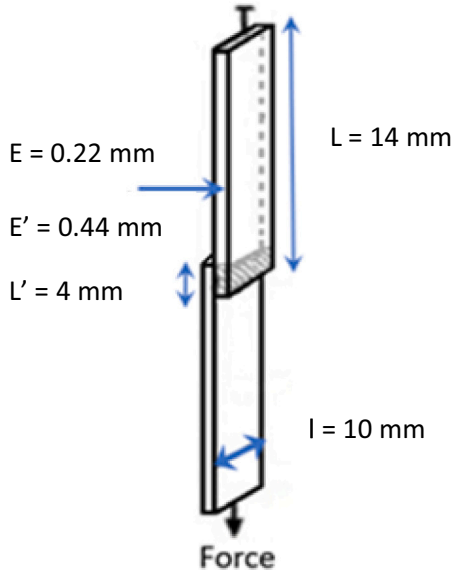

Fig. 1. Sample dimensions used for tensile tests.

3. Results and discussion

3.1. Composition of the extracts

The TCC and protein content of the samples extracted by maceration for 30 min (0%US), combination of 15 min maceration and 15 min ultrasound (50%US), ultrasound treatment for 30 min (100%US), and that obtained under optimized conditions (OP%US) are shown in Table 1. At mild conditions (25 °C), the maximum of TCC (%) is obtained for 50%US (80.2%), while the lowest value of 58.2% is obtained for 0%US. The increase of ultrasound from 50 to 100%US decreases the TTC from 80.2 to 66.1%. OP%US actually presents the highest TCC (83%) compared to 0, 50, and 100%US extracts. In fact, sonication destroys the plant cell wall and reduces the particle size, which enhances the polysaccharides extraction [25]. SEC analysis was performed to figure out the effect of ultrasound treatment on the molar mass of the extracts, as summarized in Table 1. The results indicate that the increase of ultrasound time from 0 to 30 min at mild condition 25 °C doesn't affect the molar masse. Nevertheless, excessive US treatment provokes chain cleavage due to the cavitation effects [26].

The results also show that under mild temperature (25 °C), increasing US treatment from 0% to 100% leads to protein content increase from 2.4% to 7.7%. Thus, the use of ultrasound could allow to extract additional species. It is also noted that OP%US presents the lowest proteins content of 2.1%. Similar results were reported by Hou et al. The authors obtained protein content of 1.9% and 3.7% in the extracts from Chestnut without or with ultrasound treatment, respectively [27]. Extraction was made at 80 °C for 30 min with a volume to mass ratio of 20 mL/g.

3.2. Rheological characterization

3.2.1. Analysis of linear viscoelastic domain LVE

The determination of the linear viscoelastic behavior (LVE) makes it possible to identify the gel state (G′ > G″), and liquid behavior (G′ < G″). Serrero et al. defined an intermediate state when G′ and G″ are overlapped [28].

Fig. 2 and Table 2 present the linear viscoelastic region for the 4 samples at fixed angular frequency of 10 rad/s. Different concentrations were used: 5%, 10%, and 15% for 0%US, 5%, 6.75%, 10%, and 15% for 50%US, 5%, 6.37%, 10%, and 15% for 100%US, and 10%, 20%, and 30% for OP%US, respectively. The concentrations were selected so as to find and characterize the three states, i.e., liquid, intermediate, and gel states. The single factor ANOVA test was carried out to determine the significance of difference between the values of G′ and G″. The results are presented in Tables 1S and 2S (see Supporting information).

For 0%US at 5%, the sample presents a liquid-state behavior as G″ (0.70 Pa) is higher than G′ (0.37 Pa). The p-value is 3.1 × 10^{-4}, indicating there is significant difference between G′ and G″. At a concentration of 10%, the G′ and G″ increase to 1.97 Pa and 1.96 Pa, respectively. The p-value is 9.08 × 10^{-1}, indicating that G′ and G″ are overlapped and there is no significant difference between them, characterizing the intermediate state. Indeed at 15%, the G′ and G″ values are 6.02 Pa and 4.65 Pa, respectively, with a p-value of 1.3754 × 10^{-2}. This indicates that the sample is characterized as gel state behavior.

50%US presents also a liquid sated behavior at 5%. The G′ and G″ values are 0.52 and 0.62 Pa, respectively, with a p-value of 6.142 ×

Table 1
Total carbohydrate content (TCC) and proteins content data of the extracts.

Extract	TCC (%)	Protein's content (%)	Mw	Đ
OP%US	83.0 ± 0.1	2.1 ± 0.1	–	–
0%US	58.2 ± 1.1	2.4 ± 0.1	3140	1.452
50%US	80.2 ± 1.0	4.8 ± 0.2	3235	1.467
100%US	66.1 ± 0.3	7.7 ± 0.3	3145	1.482

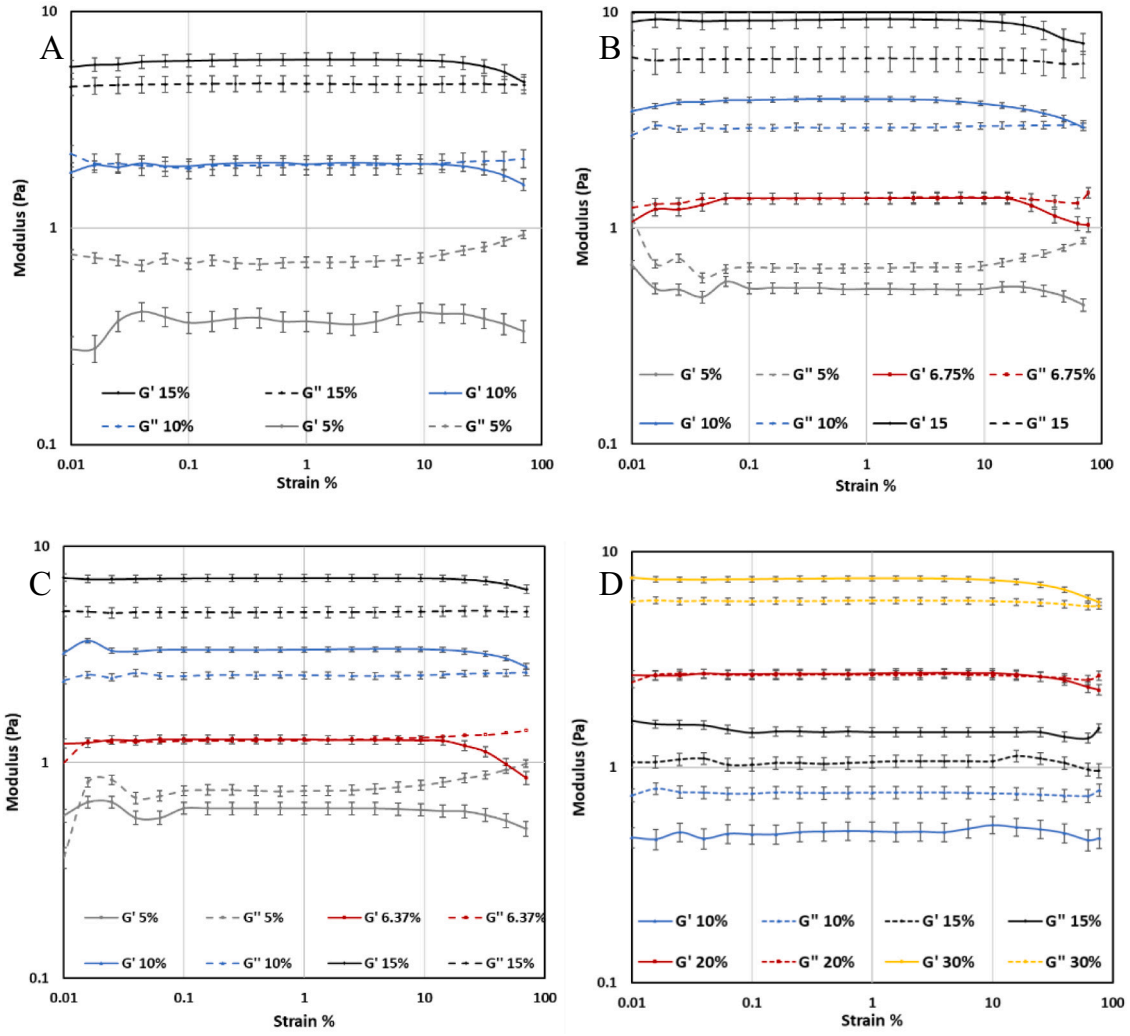

Fig. 2. Storage modulus (G′) and loss modulus (G″) changes as a function of strain: 0%US (A), 50%US (B), 100%US (C), and OP%US (D) at different concentrations.

Table 2
G′ and G″ values of 0%US, 50%US, 100% US, and OP%US from LVE tests.

LVE	0%US		50%US		100%US		OP%US	
w/v (%)	G′	G″	G′	G″	G′	G″	G′	G″
5	0.37 ± 0.04	0.696 ± 0.04	0.52 ± 0.03	0.65 ± 0.03	0.61 ± 0.04	0.74 ± 0.04	–	–
6.37	–	–	–	–	1.28 ± 0.06	1.27 ± 0.06	–	–
6.75	–	–	1.37 ± 0.08	1.38 ± 0.08	–	–	–	–
10	1.97 ± 0.1	1.96 ± 0.1	3.96 ± 0.11	2.93 ± 0.11	3.33 ± 0.09	2.53 ± 0.09	0.51 ± 0.05	0.77 ± 0.05
15	6.02 ± 0.4	4.65 ± 0.4	9.28 ± 0.8	6.1 ± 0.8	7.16 ± 0.28	4.97 ± 0.28	1.06 ± 0.07	1.46 ± 0.07
20	–	–	–	–	–	–	2.73 ± 0.13	2.69 ± 0.13
30	–	–	–	–	–	–	7.53 ± 0.21	5.95 ± 0.21

10^{-3}. The intermediate state is detected at 6.75% with G′ and G″ values 1.37 Pa, and 1.38 Pa, respectively. The p-value is 8.86×10^{-1}, indicating that there is no significant difference between G′ and G″. The solid-state behavior was observed for concentrations above 6.75%. When the concentration increases from 10% to 15% the G′ increases from 3.96 to 9.28 Pa, and the G″ increases from 2.93 to 6.1 Pa. The p-value of 10% and 15% are 8.23×10^{-3} and 4.2×10^{-5}, respectively.

The liquid state of 100%US is also detected at 5%. The G′ and G″ values are 0.61 Pa and 0.74 Pa, respectively. The p-value is 1.823×10^{-2}, in agreement with a significant difference between G′ and G″. The intermediate state is detected at a concentration of 6.37%. The values of G′ and G″ are 1.28 and 1.27 Pa, respectively, with a p-value of 0.819. When the concentration increases from 10% to 15%, the G′ and G″ increase from 3.33 to 7.16, and from 2.53 to 4.97, with p-values of 4.08×10^{-4} and 7.77×10^{-5}, respectively.

OP%US is extracted at higher temperature (45 °C) compared to 0%, 50%, and 100%US which are extracted at 25 °C. The sample presents a liquid state behavior (G″ > G′) at 10% and 15%. When the concentration increases from 10% to 15%, the G′ increases from 0.51 Pa to 1.06 Pa, and G″ from 0.77 Pa to 1.46 Pa. The p-value for 10% and 15% is 3.162×10^{-3}, and 2.194×10^{-3}, respectively, indicating a significant difference between G″ and G′. The intermediate state is detected at 20% with G′ and G″ values of 2.73 and 2.69 Pa, respectively with a p-value 7.25×10^{-1}. At 30%, the OP%US sample exhibits a gel-state behavior, with G′,

G″ and p-value of 7.53 Pa, 5.95 Pa, and 7.71 × 10^{-4}, respectively. It is noticed that 50%US presents the highest values of G′ and G″ compared to 0%, 100%, and OP%US.

Table 2S presents the results of single factor ANOVA tests for G′ and G″ carried out at the same concentration for different ultrasound treatments. The results of p-values indicate clearly that there is a significant difference for G′ at 5%, 10%, 15% w/v between (0%US, 50%US), (0% US, 100% US) and (50%US, 100% US), while there is no significant difference for G″ between (0%US, 50%US), (0%US, 100%US), and (50% US, 100%US). Therefore, the storage modulus is strongly affected by ultrasound treatment, in contrast to loss modulus. Indeed, when the temperature increases from 25 °C to 45 °C at 10%, all p-values for G′ and G″ are significant, while at 15% the p values of G″ for (50%US, OP%US), and (100%US, OP%US) are not significant. Hence, at high temperature and low concentration, the loss modulus is also affected by ultrasound treatment.

The storage modulus represents the energy stored in the elastic structure of a material or hydrogel whereas the loss modulus represents the amount of energy dissipated in the sample [29]. In other words, the storage modulus increases with the increasing of molar masse, chains entanglement, and crosslinking. Thus, longer ultrasound treatment decreases the percentage of high molar masse chains, leading to decrease of polymer chains entanglement and consequently to decrease the storage modulus.

3.2.2. *Frequency sweep analysis*

The viscoelastic behavior was studied at fixed shear stress of 1 Pa for all samples (0%US, 50%US, 100%US, and OP%US) at different concentrations, as shown in Fig. 3. Both G′ and G″ increase with the increase of concentration, and are depended on the frequency. The liquid states are detected at 5% for 0%, 50%, and 100% US, whereas the solid states are detected at 15% for 0%US, and at 10% for 50%US and 100%US. The intermediate states are detected at 10%, 6.75%, and 6.37% for 0, 50, and 100%US, respectively, in agreement with the results of LVE tests. tan δ = G″/G′ is used to characterize the viscoelastic state of hydrogels. tan δ value below 1, equal to 1, and above 1 is characteristic of solid-state, intermediate state and liquid-state, respectively. The results are presented in Table 3, together with the slopes of G′ and G″ determined from the frequency sweep tests. tan δ well corroborate with those of LVE tests. On the other hand, when the concentration increases from 5% to 15%, the slope of G′ for 0%, 50%, 100%US, and OP%US decreases from 0.946 to 0.482, from 0.546 to 0.242, from 0.659 to 0.397, and from 0.749 to 0.404, respectively. The same trend is observed for the slope of loss modulus. These findings suggest that with increasing concentration, G′ and G″ become less sensitive to frequency increase because of higher chains entanglement.

3.3. *Mechanical characterization of adhesive properties and correlation with rheological tests*

3.3.1. *Adhesive tests on the paper substrates*

The stress at break of paper was first measured in order to determine the maximum force that can be supported by the paper. A value of 1310 ± 110 kPa was obtained. The adhesive force on the papers of 0%US, 50% US, and 100%US was evaluated at different concentrations (5, 10, 15% w/v) as shown in Fig. 4. The adhesion strength is dependent on the concentration. When the latter increases from 5 to 15% w/v, the adhesion strength increases from 183.5 to 843.5 kPa, from 350.2 to 1211.5 kPa, and from 186.2 to 1146.7 kPa for 0%, 50%, and 100%US, respectively. ANOVA tests were carried out in order to determine the significance of difference between the adhesion strengths. The p-values of adhesion strength at different concentrations for all samples presented in (Table 3S Supporting information) are below 0.05, indicting a significant difference of adhesion strengths.

The adhesion strength is also dependent on the ultrasound treatment. 50%US presents the highest adhesion strength compared to 0%US and 100%US at different concentrations probably due to its high polysaccharide purity.

The p-values below 0.0001 clearly indicate that there is a significant difference of adhesion strength between 0%US and 50%US at 5%, 10%, and 15% w/v (Table 3S Supporting information). While, no significant difference is detected between 0%US and 100%US at 5% w/v, in

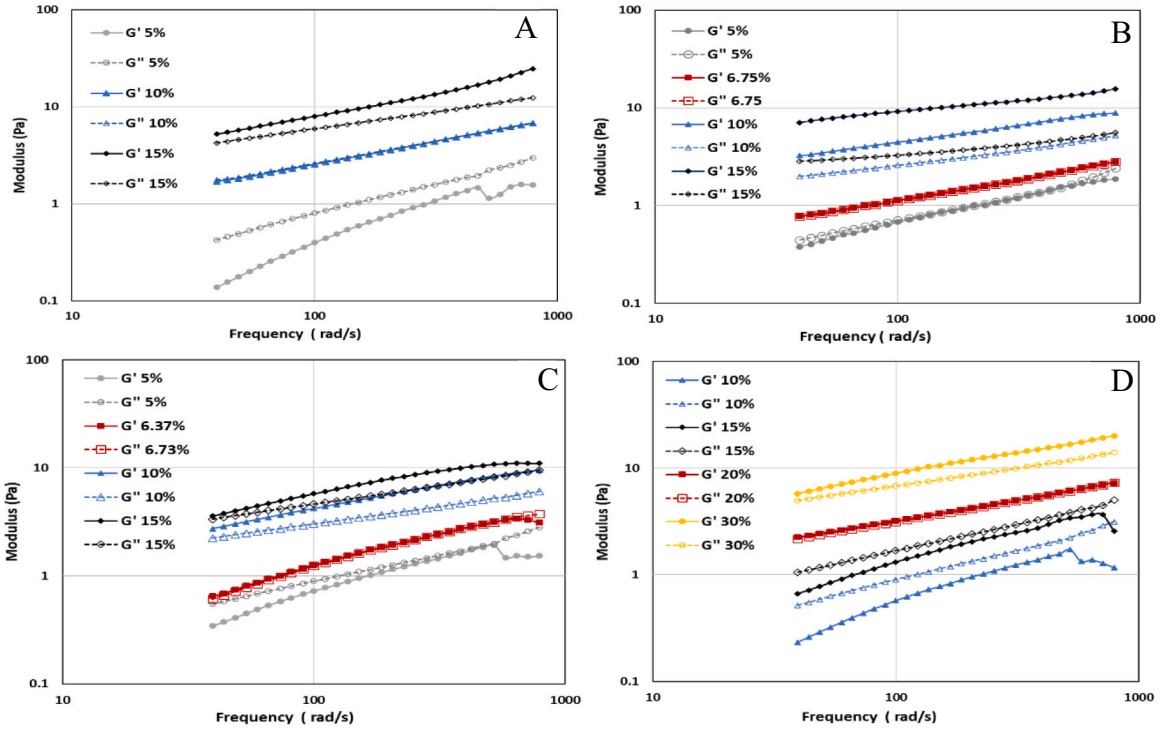

Fig. 3. Frequency sweep of 0% (A), 50% (B), 100%US (C), and OP%US (D) at different concentrations.

Table 3
Data of the slopes of G′ and G″, and tan δ calculated at low frequency range (0–6 rad/s).

w/v (%)	0%US			50%US				100%US				OP%US			
	5%	10%	15%	5%	6.75%	10%	15%	5%	6.37%	10%	15%	10%	15%	20%	30%
Slope G′	0.946	0.573	0.482	0.546	0.425	0.208	0.242	0.659	0.609	0.425	0.397	0.748	0.597	0.387	0.404
Slope G″	0.622	0.455	0.355	0.504	0.327	0.313	0.22	0.515	0.628	0.327	0.344	0.565	0.496	0.399	0.339
tan δ	3.072	1.042	0.809	1.180	0.990	0.612	0.168	1.590	0.938	0.817	0.633	2.218	1.589	0.965	0.861

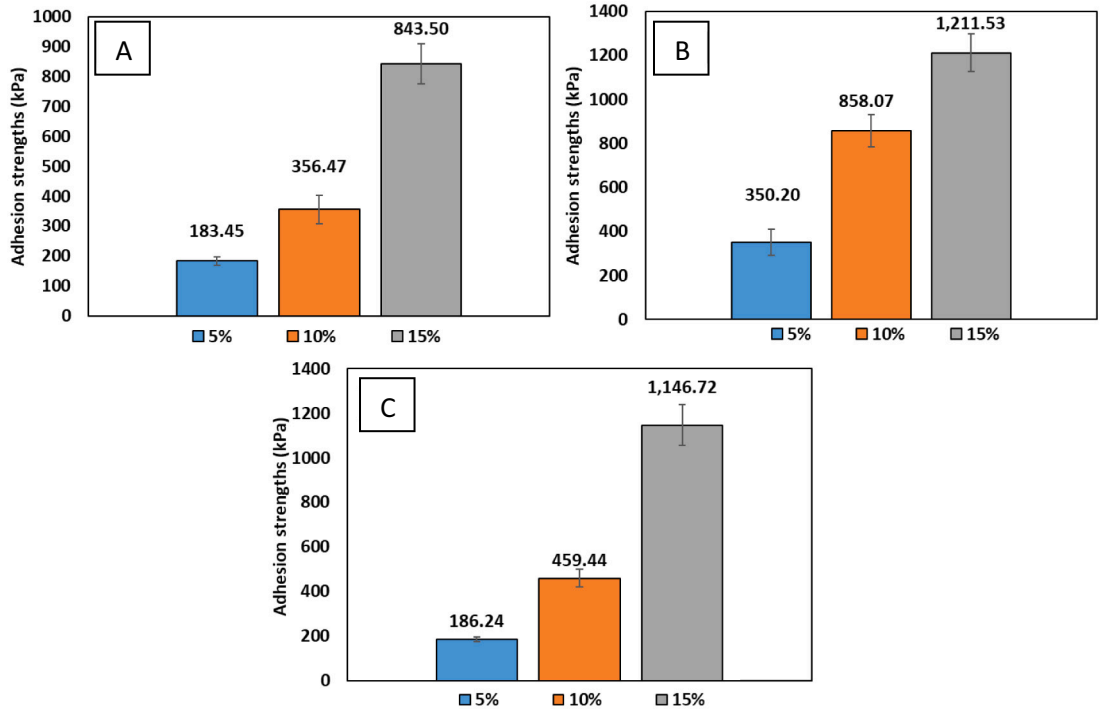

Fig. 4. Adhesion strengths (kPa) on the paper substrate for 0%US (A), 50%US (B), and 100%US (C) measured at break.

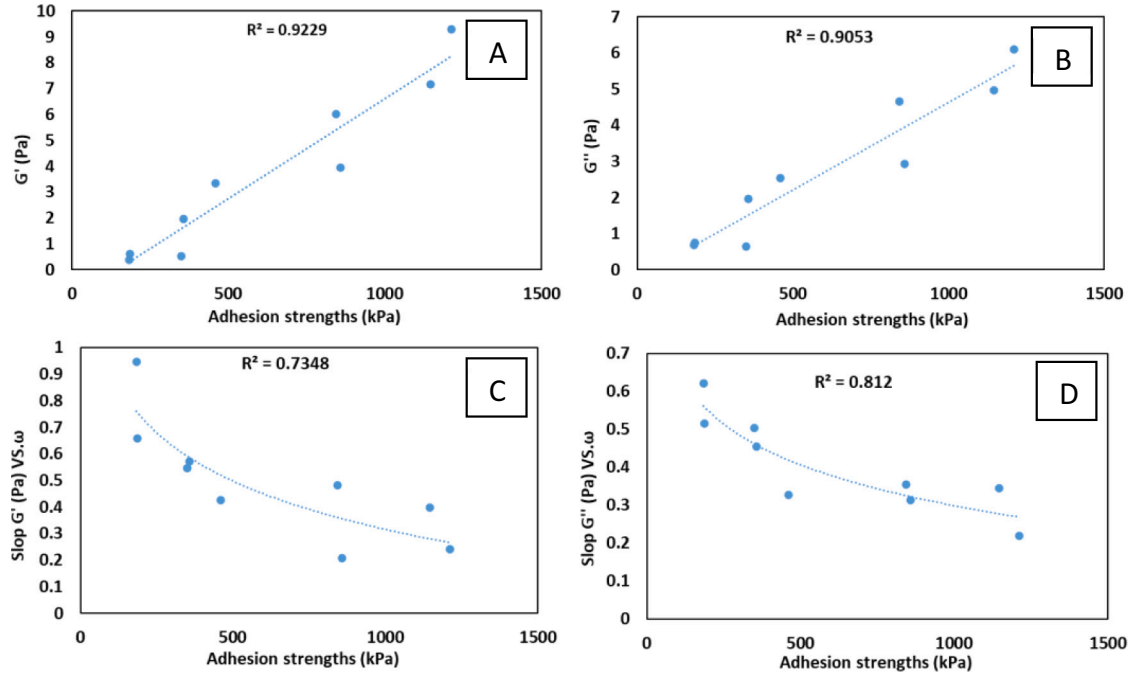

Fig. 5. Correlation analysis between rheological and adhesion strength results on the paper substrate. (A) Storage modulus (G′) vs. adhesion strength; (B), loss modulus (G″) vs. adhesion strength; (C), slope of storage modulus (G′ vs. f(ω)) vs. adhesion strength; (D), slope of loss modulus (G″ vs. f(ω)) vs. adhesion strength.

contrast to 10% and 15% w/v. Hence, the significance between 0%US and 100%US increases with increasing concentration. However, the p-values for 50%US and 100% US at 5% and 10% w/v are below 0.001, indicating a significant difference. But the p-value at 15% w/v is well above 0.05, suggesting absence of significant difference. This finding could be assigned to the fact that the adhesion strength is very close to the maximum force which can be supported by the substrate. At 15% w/v of 50%US, failure started to appear in the substrate.

The adhesion strength data can be correlated to the rheological behaviors of the adhesives. The highest values of G′ and G″ and the lowest slopes of G′ or G″ vs. f(ω) curves are indicator of high cohesion and strong adhesion [30]. The G′ and G″ data of all samples are plotted vs. adhesion strength in Fig. 5A and B. The results indicate that the increase of G′ from 0.37 to 9.28 Pa, and G″ from 0.696 to 6.1 Pa leads to increase of adhesion strength from 183.45 to 1211.53 kPa. The R^2 values are 0.923 and 0.905, respectively, showing that both G′ and G″ vs. adhesion strength are significantly linearly correlated. The results well agree with the work of Vakalopoulos et al. The authors tested 2-octyl-cyanoacrylate mixed with butyl lactoyl cyanoacylate (Omnex adhesive)/colonic serosa. The G′ and G″ values are 107 and 106 Pa, respectively, and the best adhesion strength obtained is 48 Pa. The correlation between G′ and G″ vs. adhesion strength for 12 adhesive samples yielded R^2 values of 0.711 and 0.716, respectively [30].

The slopes of G′ and G″ determined from the frequency sweep are also plotted vs. adhesion strength as shown in Fig. 5C and D. It appears that the decrease of G′ slope from 0.946 to 0.242, or that of G″ slope from 0.622 to 0.22 corresponds to increase of the adhesion strength from 183.5 to 1211.5 kPa. The R^2 values are 0.735 and 0.812 for G′ and G″ slopes vs. adhesion strength curves, respectively, suggesting a significantly logarithmic correlation. These correlations suggest that the adhesion strength could be predicted from the rheological properties.

3.3.2. *Adhesive tests on PLA substrates*

Adhesive tests were also performed on PLA substrates. Fig. 6 presents the results of adhesion strength (kPa) for 0%US, 50%US, and 100%US at different concentrations. As mentioned above (LVE tests), Three concentrations were used according to LVE tests in order to identify the effect of the sample states (liquid, intermediate, and solid states) on the adhesion strength. At 5%, all samples have a liquid state behavior, the adhesion strength is 205, 262, and 238 kPa, for 0%US, 50%US, and 100%US, respectively. When the samples are in a gel state (at a concentration of 15% for 0%US, 10% for 50%US and 100%US), the adhesion strengths are 259, 402, and 299 kPa, respectively. The best adhesion strengths of 278.23, 58.52, and 380.94 kPa are obtained in the intermediate state for 0%US, 50%US, and 100%US at a concentration of 10%, 6.75%, and 6.37% w/v, respectively. Comparison of the three samples indicates that 50%US presents better adhesion strength than 0% US and 100%US in all the three states.

ANOVA tests were carried out in order to determine the p-values of samples in different states as shown in Table 4S. The p-values for 0%US, 50%US, and 100%US between the different states are inferior to 0.001, indicating that the state of adhesives has a significant influence on the adhesion strength. ANOVA tests were also carried out in order to determine the effect of ultrasound treatment on the adhesion strength at different states of samples. The p-values presented in Table 5S are below 0.001 except that of the comparison between 50%US and 100%US at the liquid state which is 0.122. These results suggest that the ultrasound treatment has a very significant impact on the adhesion strength, especially in the intermediate state.

In order to understand the effect of rheological behavior on the adhesion strength, G′, G″, and slopes of G′ and G″ vs. f(ω) curves were plotted against the adhesion strengths (Fig. 7). It seems that there is no direct correlation between G′, G″, slope G″ vs. f(ω) and the adhesion strength tested on the PLA substrate. A week correlation is detected between slope G′ vs. f(ω) and the adhesion strength with R^2 of 0.448. When the slope G′ vs. f(ω) decreases, the adhesion strength increases.

On the other hand, it is noticed that the adhesion strength significantly increases when the adhesives switch from liquid state to intermediate state, and decreases when switching from intermediate state to gel state. In other words, at G′ = G″, the adhesives have the best adhesion strength. The results of correlation between rheological behavior and mechanical strength on the PLA substrate are in agreement with the

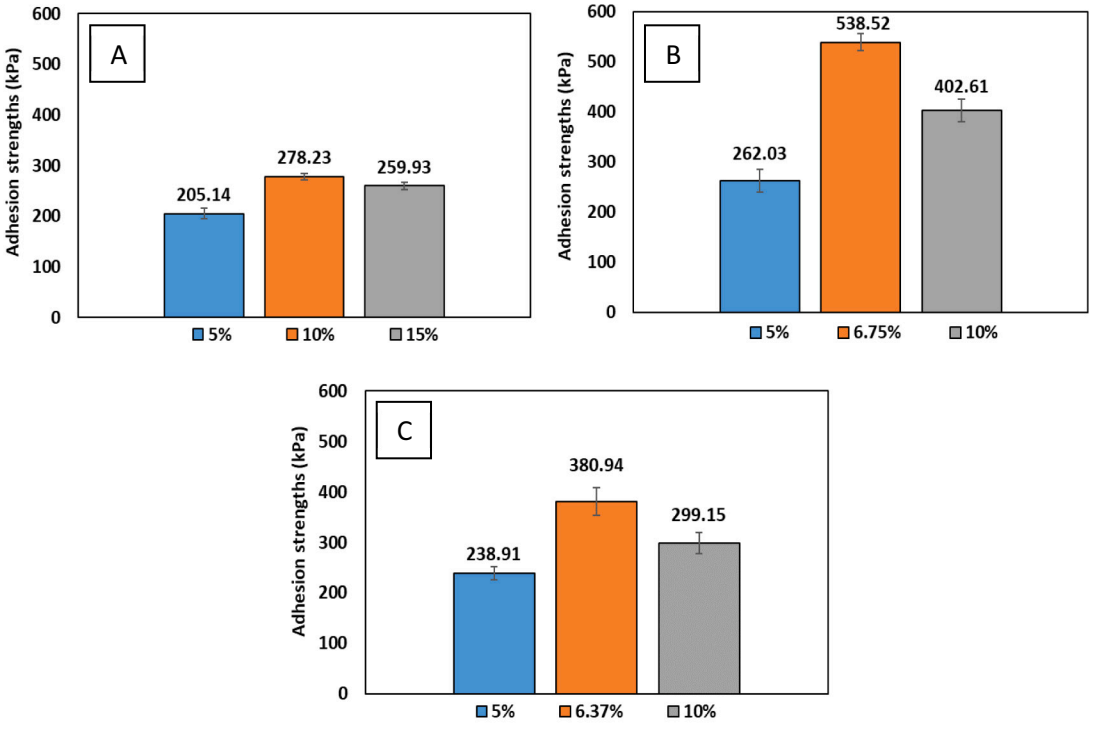

Fig. 6. Adhesion strengths (kPa) on the PLA substrate for 0%US (A), 50%US (B), and 100%US (C) measured at break.

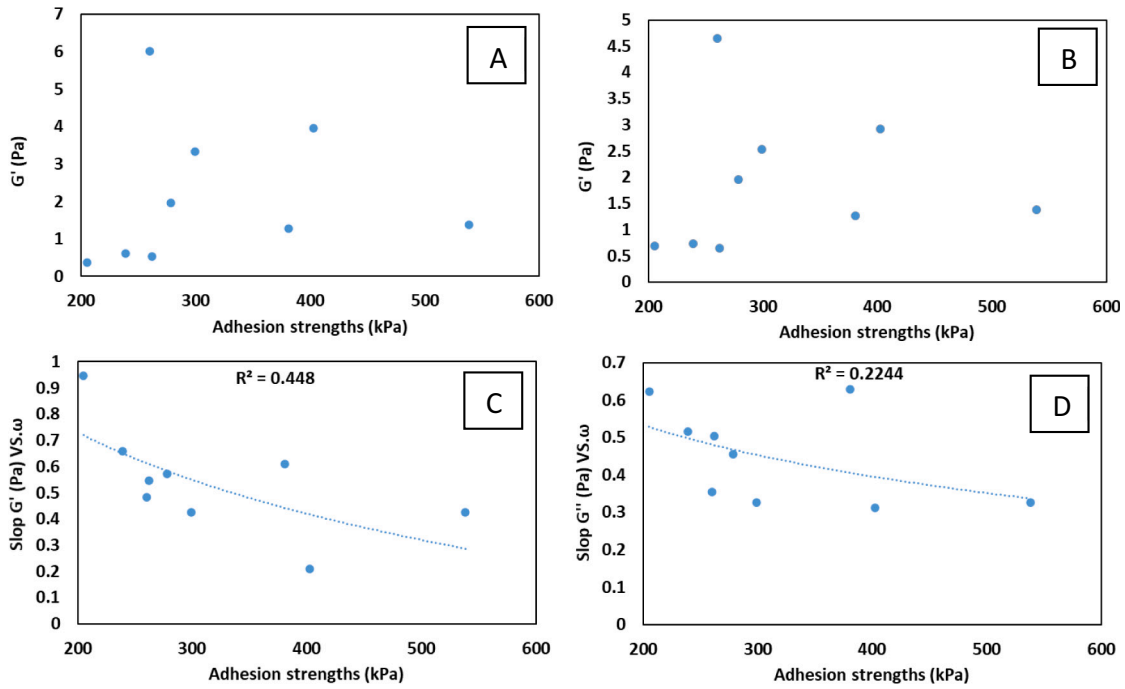

Fig. 7. Correlation analysis between rheological results vs. adhesion strengths on the PLA substrate. (A) Storage modulus (G′), (B) loss modulus (G″), (C) slope of G′ vs. f(ω), (D) slope of G″ vs. f(ω).

work reported by Serrero et al. The authors found that the adhesion strength of chitosan-based adhesives on pork skin substrate is 1.8, 4.7, and 4.1 kPa for liquid, intermediate, and gel states, respectively. It is also noted that the adhesion strength follows the same order (liquid-<gel<intermediate state) as that obtained by Serrero et al. [28].

3.3.3. *Evaluation of adhesion strength of bio-adhesive on the pork skin*

In our previous work, it was shown that the OP%US sample presents outstanding antioxidant activities and biocompatibility with a safety factor SF > 152.7 [19,20]. Thus, it is of great interest to evaluate the adhesion strength of OP%US for uses as bio-adhesive.

Firstly, the adhesion strength of OP%US was tested on the paper substrate. Increasing the concentration from 10% to 15% leads to increase the adhesion strength from 819.02 to 1418.27 kPa (Fig. 8A). At 10%, the failure occurs on the junction of the glued assembly. At this concentration, the failure is manly a cohesive failure on adhesive and substrate. But at 15%, the failure takes place on the substrate, whereas the junction remains intact (Fig. 8B). The failure is also a cohesive failure on the substrate. In other words, both the adhesive and the junction are stronger than the substrate.

The second series of tests were carried out on the skin/skin and skin/paper substrates (Fig. 9). The results clearly indicate that the adhesion strength on the skin/paper is higher than that on the skin/skin substrate. A maximum adhesion strength of 870 kPa is obtained on the skin/paper

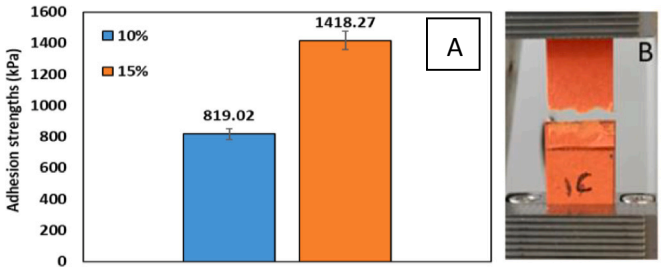

Fig. 8. (A) Adhesion strengths of OP%US at 10% and 15% on paper/paper substrate, (B) picture of cohesive failure on substrate at 15% of OP%US.

substrate at 30%, in contrast to a value of 300 kPa on the skin/skin substrate at the same concentration. This difference is assigned to the capillary force of paper which allows easy penetration of the adhesive into the micropores and asperities, a phenomenon which significantly enhances the mechanical adhesion strength. Additionally, the adhesion strength on paper/skin follows the same trend as that on the paper/paper substrate. The adhesion strength on the skin/skin substrate increases from 199.3 to 411.5 kPa when the concentration increases from 15% to 20% w/v, and then decreases to 300.71 kPa at 30%. Thus, the maximum adhesion strength is observed in the intermediate state. It is noticed that the adhesion strength on the skin/skin follows the same trend as that on PLA substrate, and that on (skin/skin) system studied by Serrero et al. [28].

ANOVA tests were carried out in order to determine the significance of difference between adhesion strengths of the reference (Velpeau) and OP%US at different concentrations (Table 6S). The p-values below 0.001 indicate a significant difference between studied systems at fixed concentrations. On the other hand, comparison is also made between the adhesion strengths of different adhesive concentrations on skin/skin and skin/paper systems (Table 7S). A significant difference is observed in all cases p-values below 0.001. Various adhesion strength values on skin substrate have been reported in literature: 4.7 ± 0.3 kPa for chitosan/oxidized starch on the pork skin substrate [28], 335 ± 88 kPa for chondroitin sulphate on the bovine membrane [31], and 1.06 ± 0.15 MPa for allyl 2-cyanoacrylate l-lactic acid reticulated adhesive on the cowhide [32]. Comparison with literature data shows that OP%US presents acceptable adhesion strength.

3.4. *Scanning electron microscopy (SEM)*

3.4.1. *SEM analysis for paper substrates*

The adhesion can be ensured by several mechanisms. In this study, there is no chemical reaction between the adhesive and the substrate. Paper has pores and micro-cavities in the structure. Additionally, paper has a micro capillary absorption which allows the penetration of adhesive in asperities and pores. Various breaking modes can be distinguished according to the location of crack during the mechanical test. In

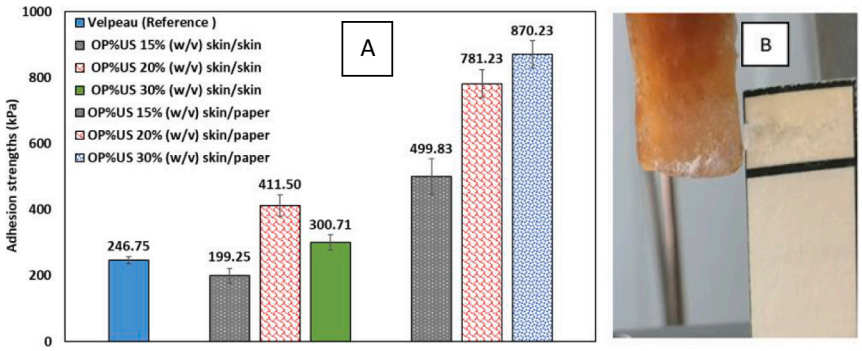

Fig. 9. (A) Adhesion strengths of OP%US at 15%, 20%, and 30% (w/v) on the skin/skin and skin/paper substrates, (B) picture of cohesive failure of OP%US at 20% (w/v) on the skin/paper substrate.

the case of cohesive failure, the failure takes place in the substrate and/or in the adhesive because of the strong adhesion strength between them. However, in adhesive failure, the failure occurs at the interface due to the weak adhesion strength between the adhesive and the substrate.

SEM was performed to observe the microscopic structure in order to identify the type of failure. Fig. 10 presents the SEM images of the substrates for samples 50%US at 5%, 10%, and 15% (w/v). At 5%, the adhesion strength is 350.2 kPa which is weaker compared to those of 10% and 15%. At this concentration the fibers of paper remain intact. In contrast, at 10% and 15%, the fibers of paper are strongly affected and cracked. The fibers appear more damaged at 15% than at 10% (w/v). The images indicate that the mode of failure is structural, and the break is present in both the adhesive and the interface (sample/paper), thus indicating that the observed failure involves a mixed mode (cohesive and adhesive).

3.4.2. *SEM analysis for PLA substrates*

SEM analysis is also performed on the failure structures for 0%US, 50%US, and 100%US at different states as shown in Fig. 11. The images for the substrate after adhesion tests indicates clearly that in liquid state, 50%US has the largest amount of adhesive on the PLA substrate. In the intermediate state, both cohesive and adhesive failure of adhesive is observed for 0%US and 100%US. In contrast, the substrate of 50%US in intermediate state presents only cohesive failure. The image also shows a strong cohesion between the adhesive and the substrate. On the other hand, at gel/solid state, the images for the substrates of 0%US and 100% US present two types of failure: adhesive and cohesive failure of adhesive. Additionally, there is a large and deep crack on the adhesive. In contrast, 50%US at gel/solid state only present cohesive failure of

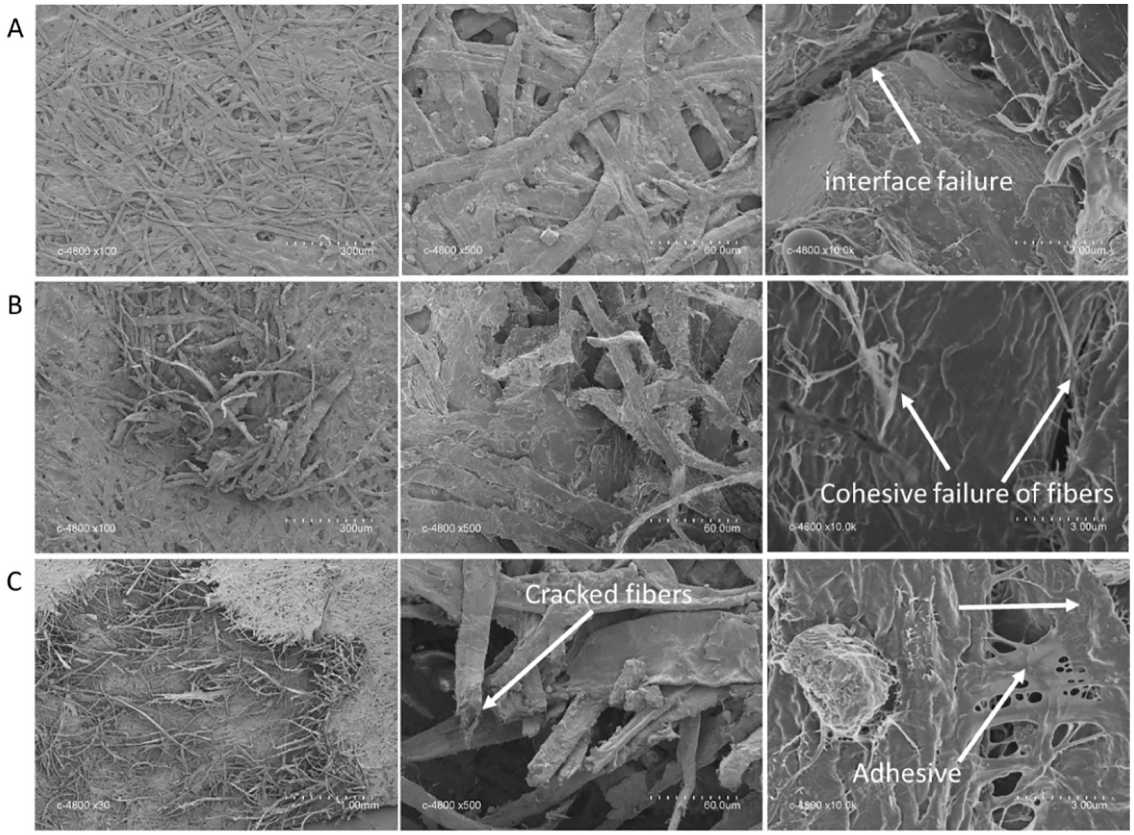

Fig. 10. SEM images at (×100, ×500, ×10,000) of the substrates (paper) after tensile tests at different concentrations of 50%US, (A) at 5%, (B) at 10%, and (C) at 15% (w/v).

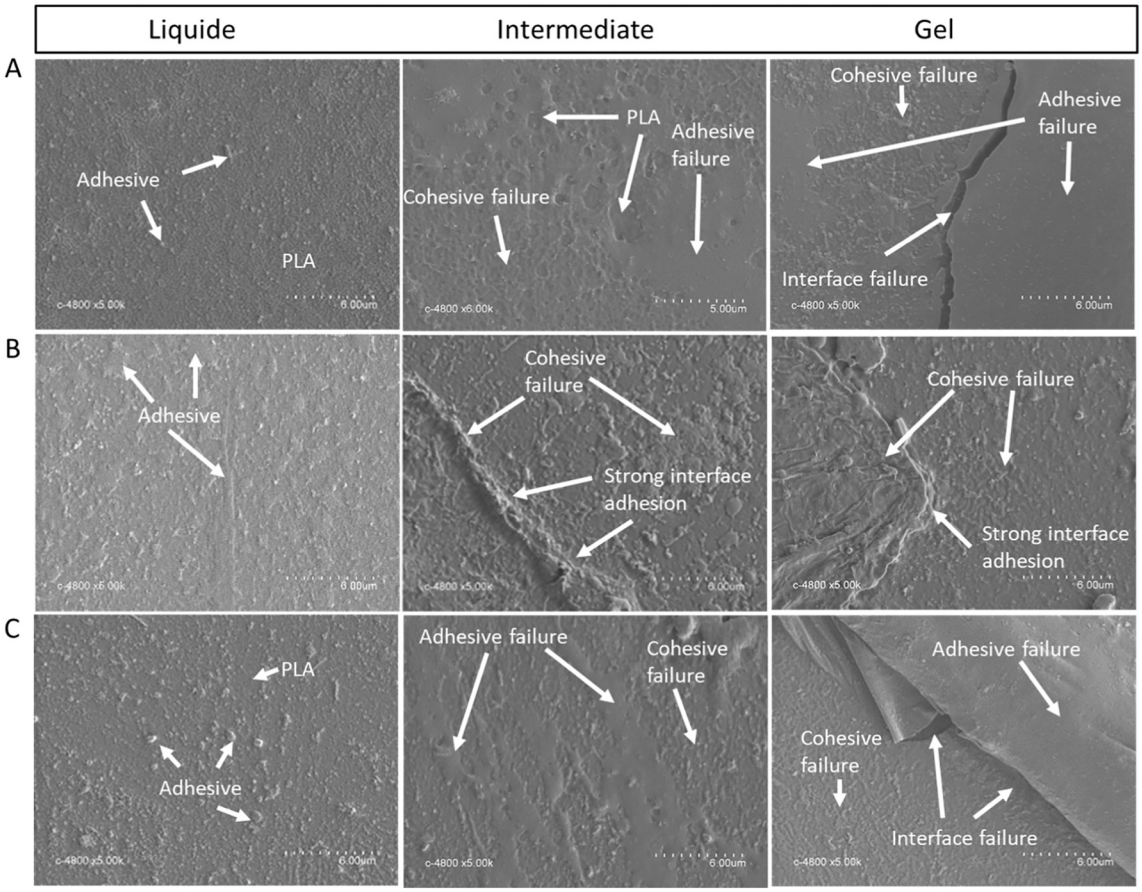

Fig. 11. SEM images of the PLA substrates after tensile tests at different adhesive states (liquid, intermediate, gel states). The series (A), (B), and (C) represent 0%US, 50%US, and 100%US, respectively.

adhesive. SEM analysis combined to the correlation between rheological states and adhesion strength may well corroborate with these two orders of adhesion strength: liquid < gel < intermediate states, and 0%US < 100%US < 50%US.

4. Conclusion

Polysaccharides are extracted from Ornithogalum under different conditions for potential uses as biobased adhesive. Analyses show that excessive ultrasound treatment affects the total carbohydrates content and proteins content of the extracts. Rheological measurements were performed to determine the liquid, intermediate and gel/solid states of the extracts, and correlated to their adhesion strength. The correlation analyses indicate that the adhesion strength is linearly correlated to G′ and G″ on the paper/paper substrate. Indeed, on PLA substrate an optimal of adhesion strength was obtained at the intermediate's states with equal storage and loss moduli due to a weak adhesion strength in liquid state, and in gel/solid state polymer chains are entrapped in the network leading to lower chain mobility and less interaction with the substrate. Comparison with literature data indicates that the extracts have a strong adhesion strength and could be very promising as a bio-based tissues adhesive for medical applications and in food packaging industry.

Suming Li, Supervision, Review & editing
Céline Pochat-Bohatier, Supervision, Review & editing.

Data availability

Data will be made available on request.

Acknowledgement

M. K. Medlej benefits of Baalbeck's municipality fellowship. The work was financially supported by Platform of Research and Analysis in Environmental Sciences (Lebanon) and by Institut Européen des Membranes (France).

References

[1] R.A. Pethrick, Composite to metal bonding in aerospace and other applications, in: Weld. Join. Aerosp. Mater, Elsevier, 2012, pp. 2012–2319, https://doi.org/10.1533/9780857095169.2.288.
[2] M.L. Mamiński, P. Borysiuk, A. Zado, Study on the water resistance of plywood bonded with UF-glutaraldehyde adhesive, Holz Als Roh-Und Werkst. 66 (2008) 469–470, https://doi.org/10.1007/s00107-008-0244-6.
[3] M. Dunky, Urea–formaldehyde (UF) adhesive resins for wood, Int. J. Adhes. Adhes. 18 (1998) 95–107, https://doi.org/10.1016/S0143-7496(97)00054-7.
[4] A.K. Patel, P. Michaud, E. Petit, H. de Baynast, M. Grédiac, J.-D. Mathias, Development of a chitosan-based adhesive. Application to wood bonding, J. Appl. Polym. Sci. 127 (2013) 5014–5021, https://doi.org/10.1002/app.38097.

[5] A.K. Patel, J.-D. Mathias, P. Michaud, Polysaccharides as adhesives, Rev. Adhes. Adhes. 1 (2013) 312–345, https://doi.org/10.7569/RAA.2013.097310.
[6] J. Li, Y. Zhang, S. Liu, J. Liu, Insights into adhesion of abalone: a mechanical approach, J. Mech. Behav. Biomed. Mater. 77 (2018) 331–336, https://doi.org/10.1016/j.jmbbm.2017.09.030.
[7] J.-L. Liu, R. Xia, A unified analysis of a micro-beam, droplet and CNT ring adhered on a substrate: calculation of variation with movable boundaries, Acta Mech. Sin. 29 (2013) 62–72, https://doi.org/10.1007/s10409-012-0202-8.
[8] V.-H. Nguyen, B.D. Nguyen, H.T. Pham, S.S. Lam, D.-V.N. Vo, M. Shokouhimehr, T. H.H. Vu, T.-B. Nguyen, S.Y. Kim, Q. Van Le, Anti-icing performance on aluminum surfaces and proposed model for freezing time calculation, Sci. Rep. 11 (2021) 3641, https://doi.org/10.1038/s41598-020-80886-x.
[9] K. Yamada, T. Chen, G. Kumar, O. Vesnovsky, L.D.T. Topoleski, G.F. Payne, Chitosan based water-resistant adhesive.Analogy to mussel glue, Biomacromolecules 1 (2000) 252–258, https://doi.org/10.1021/bm0003009.
[10] N. Mati-Baouche, C. Delattre, H. de Baynast, M. Grédiac, J.-D. Mathias, A.V. Ursu, J. Desbrières, P. Michaud, Alkyl-chitosan-based adhesive: water resistance improvement, Molecules 24 (2019) 1987, https://doi.org/10.3390/molecules24101987.
[11] C. Yuan, M. Chen, J. Luo, X. Li, Q. Gao, J. Li, A novel water-based process produces eco-friendly bio-adhesive made from green cross-linked soybean soluble polysaccharide and soy protein, Carbohydr. Polym. 169 (2017) 417–425, https://doi.org/10.1016/j.carbpol.2017.04.058.
[12] J.M. Maia, Thermo-rheological behavior of model protein – polysaccharide mixtures, 2010, https://doi.org/10.1007/s00397-010-0431-3.
[13] T. Hjertberg, J.-E. Lakso, Functional group efficiency in adhesion between polyethylene and aluminum, J. Appl. Polym. Sci. 37 (1989) 1287–1297, https://doi.org/10.1002/app.1989.070370512.
[14] V.L. Vakula, H. Yun-tsui, V.E. Gul, S.S. Voyutskiĭ, Adhesion of high polymers. VI. The effect of molecular weight of NBR copolymers of various polarities on adhesion to polar and nonpolar materials, Rubber Chem. Technol. 34 (1961) 562–570, https://doi.org/10.5254/1.3540228.
[15] S. Cui, C. Liu, Z. Wang, X. Zhang, S. Strandman, H. Tenhu, Single molecule force spectroscopy on polyelectrolytes: effect of spacer on adhesion force and linear charge density on rigidity, Macromolecules 37 (2004) 946–953, https://doi.org/10.1021/ma0353991.
[16] E. Raphael, P.G. De Gennes, Rubber-rubber adhesion with connector molecules, J. Phys. Chem. 96 (1992) 4002–4007, https://doi.org/10.1021/j100189a018.
[17] Severian Dumitriu, Polysaccharides: Structural Diversity And Functional Versatility, Second Edition, CRC Press, 270 Madison Avenue, New York, NY 10016, U.S.A., 2004.
[18] J.-D. Mathias, M. Grédiac, P. Michaud, Bio-based adhesives, in: Biopolym. Biotech Admixtures Eco-Efficient Constr. Mater, Elsevier, 2016, pp. 369–385, https://doi.org/10.1016/B978-0-08-100214-8.00016-6.
[19] M.K. Medlej, B. Cherri, G. Nasser, F. Zaviska, A. Hijazi, S. Li, C. Pochat-Bohatier, Optimization of polysaccharides extraction from a wild species of Ornithogalum combining ultrasound and maceration and their anti-oxidant properties, Int. J. Biol. Macromol. 161 (2020) 958–968, https://doi.org/10.1016/j.ijbiomac.2020.06.021.
[20] M.K. Medlej, C. Batoul, H. Olleik, S. Li, A. Hijazi, G. Nasser, M. Maresca, C. Pochat-Bohatier, Antioxidant activity and biocompatibility of fructo-polysaccharides extracted from a wild species of Ornithogalum from Lebanon, Antioxidants 10 (2021) 68, https://doi.org/10.3390/antiox10010068.
[21] M. DuBois, K.A. Gilles, J.K. Hamilton, P.A. Rebers, F. Smith, Colorimetric method for determination of sugars and related substances, Anal. Chem. 28 (1956) 350–356, https://doi.org/10.1021/ac60111a017.
[22] O.H. Lowry, N.J. Rosebrough, A.L. Farr, R.J. Randall, Protein measurement with the folin phenol reagent, J. Biol. Chem. 193 (1951) 265–275.
[23] C.S.I.S. Reproduction, (ISO 4587 : 2003 , IDT) Adhesives – Determination of tensile lap-shear strength of rigid-to-rigid bonded assemblies. https://www.sis.se/std-35031, 2004.
[24] S. Materials, Standard Test Method for Strength Properties of Tissue Adhesives in Tension 1, 2011, https://doi.org/10.1520/F2258-05R10.2.
[25] Y. Wang, C. Wang, M. Guo, Effects of ultrasound treatment on extraction and rheological properties of polysaccharides from Auricularia cornea var. Li, Molecules 24 (2019), https://doi.org/10.3390/molecules24050939.
[26] A. Ebringerová, Z. Hromádková, An overview on the application of ultrasound in extraction, separation and purification of plant polysaccharides, Open Chem. 8 (2010) 243–257, https://doi.org/10.2478/s11532-010-0006-2.
[27] F. Hou, Y. Wu, L. Kan, Q. Li, S. Xie, J. Ouyang, Effects of ultrasound on the physicochemical properties and antioxidant activities of chestnut polysaccharide, Int. J. Food Eng. 12 (2016) 439–449, https://doi.org/10.1515/ijfe-2015-0377.
[28] A. Serrero, S. Trombotto, Y. Bayon, P. Gravagna, S. Montanari, L. David, Polysaccharide-based adhesive for biomedical applications: correlation between rheological behavior and adhesion, Biomacromolecules 12 (2011) 1556–1566, https://doi.org/10.1021/bm101505r.
[29] H.A. Barnes, Rheology: principles, measurements and applications, Powder Technol. 86 (1996) 313, https://doi.org/10.1016/S0032-5910(96)90008-X.
[30] K.A. Vakalopoulos, Z. Wu, L. Kroese, G.-J. Kleinrensink, J. Jeekel, R. Vendamme, D. Dodou, J.F. Lange, Mechanical strength and rheological properties of tissue adhesives with regard to colorectal anastomosis, Ann. Surg. 261 (2015) 323–331, https://doi.org/10.1097/SLA.0000000000000599.
[31] J.A. Simson, I.A. Strehin, B.W. Allen, J.H. Elisseeff, Bonding and fusion of meniscus fibrocartilage using a novel chondroitin sulfate bone marrow tissue adhesive, Tissue Eng. Part A 19 (2013) 1843–1851, https://doi.org/10.1089/ten.tea.2012.0578.
[32] Y.J. Lee, H.S. Son, G.B. Jung, J.H. Kim, S. Choi, G.-J. Lee, H.-K. Park, Enhanced biocompatibility and wound healing properties of biodegradable polymer-modified allyl 2-cyanoacrylate tissue adhesive, Mater. Sci. Eng. C. 51 (2015) 43–50, https://doi.org/10.1016/j.msec.2015.02.042.